A Thesis

for the Degree of Master of Science in Medicine

Hyperoside protects V79-4 lung fibroblast cells against oxidative stress-induced apoptosis via inhibiting reactive oxygen species and c-Jun N-terminal kinase pathway

Mei-Jing Piao

Department of Medicine

GRADUATE SCHOOL

CHEJU NATIONAL UNIVERSITY

February, 2008

활성 산소종 및 c-Jun N-terminal 키나아제 통로의 억제를 통하여 산화적 스트레스로 유도되는 V79-4 햄스터 폐 섬유아세포의 세포사멸에 대한 Hyperoside의 보호작용

지도교수 현 진 원

박 미 경

이 논문을 의학 석사학위 논문으로 제출함

2008년 2월

박미경의 의학 석사학위 논문을 인준함

심사위원장 고윤제 ㊞

위 원 홍희경 ㊞

위 원 현진원 ㊞

제주대학교 대학원

2008년 2월

Hyperoside protects V79-4 lung fibroblast cells against oxidative stress-induced apoptosis via inhibiting reactive oxygen species and c-Jun N-terminal kinase pathway

Mei-Jing Piao

(Supervised by professor Jin-Won Hyun)

A thesis submitted in partial fulfillment of the requirement for the degree of Master of Science in Medicine

2008 . 2 .

This thesis has been examined and approved.

Moonjae Cho

Ideekyoung Kang

Jin Won Hyun

Dec. 11, 2007

Department of Medicine

GRADUATE SCHOOL

CHEJU NATIONAL UNIVERSITY

ABSTRACT

This study is to elucidate the cytoprotective effect of hyperoside (quercetin-3-D-galactoside) against hydrogen peroxide (H_2O_2) induced apoptosis and its underlying mechanisms. Hyperoside was found to scavenge intracellular reactive oxygen species (ROS), and increase catalase activity. Thereby hyperoside prevented lipid peroxidation and DNA damage, showing inhibition of thiobarbituric acid reactive substance (TBARS) formation, inhibition of comet tail, decreased phospho-H2A.X expression, and inhibition of 8-hydroxy-2′-deoxyguanosine (8-OHdG) formation. Hyperoside protects cell death of Chinese hamster lung fibroblast (V79-4) cells via inhibition of apoptosis induced by H_2O_2 as shown by decreased apoptotic nuclear fragmentation, decreased sub-G_1 cell population, decreased DNA fragmentation, inhibited mitochondria membrane potential ($\Delta\psi$) loss. The protective effects were also accompanied by up-regulation of bcl-2, down-regulation of bax, and the inactivation of caspase 9, and 3. Hyperoside abrogated the activation of c-Jun N-terminal kinase (JNK), an apoptosis related signal pathway, and its downstream transcription factor, activator protein-1 (AP-1). Taken together, these findings suggest that hyperoside protected H_2O_2 induced apoptosis of V79-4 cells by inhibiting ROS generation and JNK activation.

Keywords: *Hyperoside*; Reactive oxygen species; Apoptosis; c-Jun N-terminal kinase.

CONTENTS

LIST OF FIGURES

Ⅰ. INTRODUCTION

Reactive oxygen species (ROS) are known to cause oxidative modification of DNA, proteins, lipids and small intracellular molecules. Lipid, including pulmonary surfactant, reacts with ROS to produce lipid peroxides, which cause increased membrane permeability, inactivation of surfactant, and inhibition of normal cellular enzyme processes (Yang *et al*., 2007). Proteins reacting with ROS lead to decreased protein synthesis due to ribosomal translocation or destruction of proteins, resulting in impaired cellular metabolism and accumulation of cellular waste products (Tuder *et al*., 2003). ROS cause damage to nucleic acids by modified purine and pyrimidine base and DNA strand breakage (Dizdaroglu *et al*., 2002). These pathological alterations by ROS may be attributed to changes in the intracellular mitogen activated protein kinase (MAPK) signaling mechanisms and three subfamily of MAPK that are sensitive to ROS have been identified: extracellular signal regulated kinase (ERK), c-Jun N-terminal kinase (JNK), and p38 kinase (Ishikawa *et al*., 1997; Abe and Berk, 1998). For example, H_2O_2 induces apoptosis of mesangial cells via the JNK pathway and the ERK pathway (Kitamura *et al*., 2002). In PC 12 rat pheochromocytoma cells, H_2O_2 stimulates rapid and significant activation of ERK, JNK and p38 kinase and JNK was more sensitive to H_2O_2 (Yoshizumi *et al*., 2002).

Hyperoside (quercetin-3-D-galactoside) is a flavonoid compound, which can be mainly found from *hypericum perforatum L.* (Zou *et al*., 2004), and possesses many properties including serine protease inhibitory effect (Jedinak *et al*., 2006), inhibition of glucose uptake (Cermak *et al*., 2004), inhibition of nitric oxide synthase (Luo *et al*., 2004), antioxidant activity (Zou *et al*., 2004), antifungal activity (Li *et al*., 2005), antiviral activity (Chen *et al*.,

2006; Wu *et al*., 2007), cardioprotective effect (Trumbeckaite *et al*., 2006), antidepressant activity (Prenner *et al*., 2007), epidermal growth factor receptor inhibitory property (Kern *et al*., 2005), and neuroprotective effect (Liu *et al*., 2005). Recently it was reported that hyperoside had a protective effect against oxidative stress induced PC 12 rat pheochromocytoma cells damage (Liu *et al*., 2005). However, the precise mechanisms of the cytoprotective effect of hyperoside against oxidative stress have not been elucidated. Oxidative stress induced by the overproduction of ROS in the lung is caused by many clinical conditions; asthma, cystic fibrosis, ischemia-reperfusion injury, drug-induced lung toxicity, cancer, and aging (Morris and Bernard, 1994; Haddad, 2002; Nguyen et al., 2003). In the present study, we report the protective effect of hyperoside on cell damage induced by hydrogen peroxide in Chinese hamster lung fibroblast (V79-4) cells and the likely protective mechanisms.

Ⅱ. MATERIALS AND METHODS

1. *Reagents*

Hyperoside (Quercetin-3-D-galactoside, Fig. 1) compound was purchased from Fluka Co. (Buchs, Switzerland). The 1,1-diphenyl-2-picrylhydrazyl (DPPH) radical, 2',7'-dichlorodihydrofluorescein diacetate (DCF-DA), and Hoechst 33342 were purchased from the Sigma Chemical Company (St. Louis, MO, USA), and thiobarbituric acid from BDH Laboratories (Poole, Dorset, UK). Primary anti-JNK, anti-phospho JNK, anti-ERK, anti-phospho ERK, anti-p38, and anti-phospho p38 antibodies were purchased from Cell Signaling Technology (Beverly, MA, USA), primary anti-catalase antibody from Biodesign International Company (Saco, Maine, USA), and primary anti-phospho histone H2A.X antibody from Upstate Biotechnology (Lake Placid, NY, USA). The plasmid containing the AP-1 binding site-luciferase construct was a generous gift of Dr. Young Joon Surh (Seoul National University, Seoul, Korea).

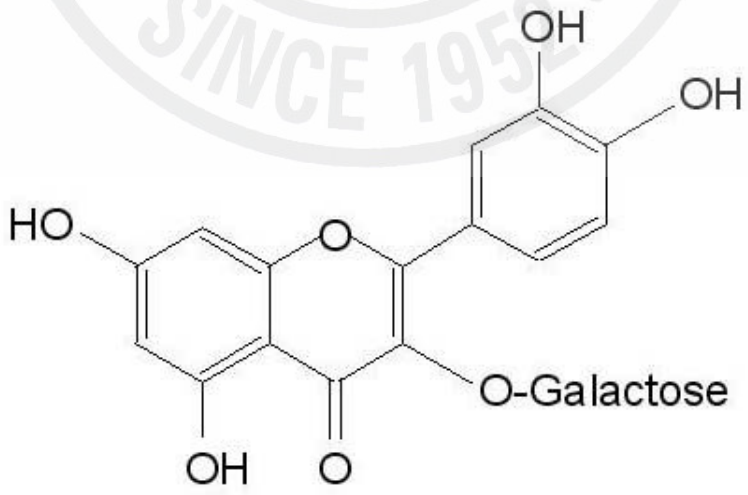

Fig. 1. Chemical structure of hyperoside (quercetin-3-D-galactoside).

2. *Cell culture*

The Chinese hamster lung fibroblast cells (V79-4) were obtained from the American Type Culture Collection. The V79-4 cells were maintained at 37℃ in an incubator, with a humidified atmosphere of 5% CO_2, and cultured in Dulbecco's modified Eagle's medium containing 10% heat-inactivated fetal calf serum, streptomycin (100 μg/ml) and penicillin (100 units/ml).

3. *Intracellular reactive oxygen species (ROS) measurement*

The DCF-DA method was used to detect the levels of intracellular ROS (Rosenkranz *et al*., 1992). The V79-4 cells were seeded in a 96 well plate at 2×10^4 cells/well. At sixteen hours after plating, the cells were treated with hyperoside at 1, 2.5, and 5 μM, and 30 min later, 1 mM H_2O_2 was added to the plate. The cells were incubated for an additional 30 min at 37℃. After addition of 25 μM of DCF-DA solution for 10 min, the fluorescence of 2',7'-dichlorofluorescein was detected using a Perkin Elmer LS-5B spectrofluorometer and using flow cytometry (Becton Dickinson, Mountain View, CA, USA), respectively. The intracellular ROS scavenging activity (%) was calculated as [(optical density of H_2O_2 treatment) – (optical density of hyperoside + H_2O_2 treatment)] / (optical density of H_2O_2 treatment) × 100. For image analysis for generation of intracellular ROS, the cells were seeded on cover-slip loaded six well plate at 2×10^5 cells/well. At sixteen hours after plating, the cells were treated with hyperoside at 5 μM and 30 min later, 1 mM H_2O_2 was added to the plate. After changing the media, 100 μM of DCF-DA was added to each well and was incubated for an additional 30 min at 37℃. After washing with PBS, the stained cells were mounted onto microscope slide in mounting medium (DAKO, Carpinteria, CA, USA). Images were collected using the Laser Scanning Microscope 5 PASCAL program (Carl Zeiss,

Jena, Germany) on a confocal microscope.

4. *Western blot*

The cells were harvested, and washed twice with PBS. The harvested cells were then lysed on ice for 30 min in 100 μl of a lysis buffer [120 mM NaCl, 40 mM Tris (pH 8), 0.1% NP 40] and centrifuged at 13,000 × g for 15 min. Supernatants were collected from the lysates and protein concentrations were determined. Aliquots of the lysates (40 μg of protein) were boiled for 5 min and electrophoresed in 10% sodium dodecysulfate-polyacrylamide gel. Blots in the gels were transferred onto nitrocellulose membranes (Bio-Rad), which were then incubated with primary antibodies. The membranes were further incubated with secondary immunoglobulin-G-horseradish peroxidase conjugates (Pierce). Protein bands were detected using an enhanced chemiluminescence Western blotting detection kit (Amersham, Little Chalfont, Buckinghamshire, UK), and then exposed to X-ray film.

5. *Catalase activity*

The cells were seeded at 1×10^5 cells/ml, and at 16 h after plating, the cells were treated with hyperoside for 3 h. The harvested cells were suspended in 10 mM phosphate buffer (pH 7.5) and then lysed on ice by sonication twice for 15 sec. Triton X-100 (1%) was then added to the lysates which was further incubated for 10 min on ice. The lysates were centrifuged at 5,000 × g for 30 min at 4℃ to remove the cellular debris and the protein content was determined. For detection catalase activity, fifty μg of protein was added to 50 mM phosphate buffer (pH 7) containing 100 mM (v/v) H_2O_2. The reaction mixture was incubated for 2 min at 37℃ and absorbance monitored at 240 nm for 5 min. Changes in absorbance

with time was proportional to the breakdown of H_2O_2. Catalase activity was expressed as units/mg protein where one unit of enzyme activity was defined as the amount of enzyme required to breakdown of 1 μM H_2O_2 (Carrillo *et al*.,1991).

6. *Lipid peroxidation assay*

Lipid peroxidation was assayed by the thiobarbituric acid reaction (Ohkawa *et al*., 1979). The cells were then washed with cold phosphate buffered saline (PBS), scraped and homogenized in ice-cold 1.15% KCl. One hundred μl of the cell lysates was mixed with 0.2 ml of 8.1% sodium dodecylsulfate, 1.5 ml of 20% acetic acid (adjusted to pH 3.5) and 1.5 ml of 0.8% thiobarbituric acid (TBA). The mixture was made up to a final volume of 4 ml with distilled water and heated to 95℃ for 2 h. After cooling to room temperature, 5 ml of n-butanol and pyridine mixture (15:1, v/v) was added to each sample, and the mixture was shaken. After centrifugation at 1,000 × g for 10 min, the supernatant fraction was isolated, and the absorbance measured spectrophotometrically at 532 nm. Amount of thiobarbituric acid reactive substance (TBARS) was determined using standard curve with 1,1,3,3,-tetrahydroxypropane.

7. *Comet assay*

A Comet assay was performed to assess oxidative DNA damage (Singh, 2000; Rajagopalan *et al*., 2003). The cell pellet (1.5×10^5 cells) was mixed with 100 μl of 0.5% low melting agarose (LMA) at 39℃ and spread on a fully frosted microscopic slide that was pre-coated with 200 μl of 1% normal melting agarose (NMA). After solidification of the agarose, the slide was covered with another 75 μl of 0.5% LMA and then immersed in lysis solution (2.5 M NaCl, 100 mM Na-EDTA, 10 mM Tris, 1% Trion X-100, and 10% DMSO,

pH 10) for 1 h at 4℃. The slides were then placed in a gel-electrophoresis apparatus containing 300 mM NaOH and 10 mM Na-EDTA (pH 13) for 40 min to allow DNA unwinding and the expression of the alkali labile damage. An electrical field was applied (300 mA, 25 V) for 20 min at 4℃ to draw negatively charged DNA toward an anode. After electrophoresis, the slides were washed three times for 5 min at 4℃ in a neutralizing buffer (0.4 M Tris, pH 7.5) and then stained with 75 μl of ethidium bromide (20 μg/ml). The slides were observed using a fluorescence microscope and image analysis (Komet, Andor Technology, Belfast, UK). The percentage of total fluorescence in the tail and the tail length of the 50 cells per slide were recorded.

8. *Immunocytochemistry*

Cells plated on coverslips were fixed with 4% paraformaldehyde for 30 min and permeabilized with 0.1% Triton X-100 in PBS for 2.5 min. Cells were treated with blocking medium (3% bovine serum albumin in PBS) for 1 h and incubated with anti- phospho histone H2A.X antibody diluted in blocking medium for 2 h. Immunoreactive primary phospho histone H2A.X antibody was detected by a 1:500 dilution of FITC-conjugated secondary antibody (Jackson ImmunoResearch Laboratories, West Glove, PA, USA) for 1 h. After washing with PBS, the stained cells were mounted onto microscope slides in mounting medium with DAPI (Vector, Burlingame, CA, USA). Images were collected using the Laser Scanning Microscope 5 PASCAL program (Carl Zeiss, Jena, Germany) on a confocal microscope.

9. *8-Hydroxy-2'-deoxyguanosine (8-OHdG) assay*

8-OHdG amount in DNA was determined using Bioxytech 8-OHdG-ELISA Kit purchased

from OXIS Health Products following the manufacturer's instructions. Cellular DNA was isolated using DNAzol reagent (Life Technologies, Grand Island, NY, USA) and quantified using a spectrophotometer.

10. *Cell viability*

The effect of hyperoside on the viability of the V79-4 cells was determined using the [3-(4,5-dimethylthiazol-2-yl)-2,5-diphenyltetrazolium] bromide (MTT) assay (Carmichael *et al*., 1987). Fifty μl of the MTT stock solution (2 mg/ml) was then added into each well to attain a total reaction volume of 200 μl. After incubating for 4 h, the plate was centrifuged at 800 × g for 5 min and the supernatants were aspirated. The formazan crystals in each well were dissolved in 150 μl of dimethylsulfoxide and read at A_{540} on a scanning multi-well spectrophotometer.

11. *Nuclear staining with Hoechst 33342*

1.5 μl of Hoechst 33342 (stock 10 mg/ml), a DNA specific fluorescent dye, was added to each well (1.5 ml) and incubated for 10 min at 37℃. The stained cells were then observed under a fluorescent microscope, which was equipped with a CoolSNAP-Pro color digital camera, in order to examine the degree of nuclear condensation.

12. *Flow cytometry analysis*

Flow cytometry was performed to determine the content of apoptotic sub G_1 hypo-diploid cells (Nicoletti *et al*., 1991). The cells were harvested, and fixed in 1 ml of 70% ethanol for 30 min at 4℃. The cells were washed twice with PBS, and then incubated for 30 min in dark at 37℃ in 1 ml of PBS containing 100 μg propidium iodide and 100 μg RNase A. Flow

cytometric analysis was performed using a FACSCalibur flow cytometer (Becton Dickinson, San Jose, CA, USA). The proportion of sub G_1 hypo-diploid cells was assessed by the histograms generated using the computer program, Cell Quest and Mod-Fit.

13. *DNA fragmentation*

Cellular DNA-fragmentation was assessed by analysis of the cytoplasmic histone-associated DNA fragmentation using a kit from Roche Diagnostics (Mannheim, German) according to the manufacturer's instructions.

14. *Mitochondria membrane potential (Δψ) analysis*

The cells were harvested, washed and suspended in PBS containing JC-1 (10 μg/ml). After 15 min of incubation at 37℃, cells were washed, suspended in PBS, and analyzed by flow cytometer (Madge *et al*., 2003).

15. *Preparation of nuclear extract and electrophoretic mobility shift assay*

The cells were harvested, and were then lysed on ice with 1 ml of lysis buffer (10 mM Tris-HCl, pH 7.9, 10 mM NaCl, 3 mM $MgCl_2$, and 1% NP-40) for 4 min. After 10 min of centrifugation at 3,000 × g, the pellets were resuspended in 50 μl of extraction buffer (20 mM HEPES, pH 7.9, 20% glycerol, 1.5 mM $MgCl_2$, 0.2 mM EDTA, 1 mM DTT, and 1 mM PMSF), incubated on ice for 30 min, and centrifuged at 13,000 × g for 5 min. The supernatant (nuclear protein) stored at –70℃ after determination of protein concentration. Oligonucleotides containing the transcription factor AP-1 consensus sequence (5'- CGC TTG ATG ACT CAG CCG GAA - 3') were annealed, labeled with [γ-^{32}P] ATP using T4 polynucleotide kinase, and used as probes. The probes (50,000 cpm) were incubated with 6

μg of the nuclear extracts at 4℃ for 30 min in a final volume of 20 μl containing 12.5% glycerol, 12.5 mM HEPES (pH 7.9), 4 mM Tris-HCl (pH 7.9), 60 mM KCl, 1 mM EDTA, and 1 mM DTT with 1 μg of poly (dI-dC). Binding products were resolved on 5% polyacrylamide gel and the bands were visualized by autoradiography.

16. *Transient transfection and AP-1 luciferase assay*

The cells were transiently transfected with the plasmid harboring the AP-1 promoter using DOTAP as the transfection reagent according to the instructions given by the manufacturer (Roche Diagnostics). After overnight transfection, the cells were treated with 5 μM of hyperoside. After a further incubation for 1 h, 1 mM H_2O_2 was added to the culture. After 3 h, the cells were then washed twice with PBS and lysed with reporter lysis buffer (Promega, Madison, Wisconsin, USA). After vortex-mixing and centrifugation at 12,000 × g for 1 min at 4℃, the supernatant was stored –70℃ for the luciferase assay. After 20 μl of the cell extract was mixed with 100 μl of the luciferase assay reagent at room temperature, the mixture was placed in a illuminometer to measure the light produced.

17. *Statistical analysis*

All the measurements were made in triplicate and all values were represented as means ± standard error (SE). The results were subjected to an analysis of the variance (ANOVA) using the Tukey test to analyze the differences. $p<0.05$ were considered to be significant.

Ⅲ. RESULTS

1. *Effect of hyperoside on ROS scavenging activity and catalase activity*

The intracellular ROS scavenging activity of hyperoside was 30% at 1 μM, 70% at 2.5 μM, and 84% at 5 μM. (Fig. 2A). The fluorescence intensity of DCF-DA staining was also measured using flow cytometer and confocal microscope. The level of ROS detected using flow cytometer (Fig. 2B) showed 422 value of fluorescence intensity which was produced from ROS stained by DCF-DA fluorescence dye in H_2O_2+ hyperoside (5 μM) treated cells compared to 527 value of fluorescence intensity in H_2O_2 treated cells. Confocal microscopic analysis showed that hyperoside reduced the red fluorescence intensity upon H_2O_2 treatment as shown in Fig. 2C, thus reflecting a reduction in ROS generation. To investigate whether the radical scavenging activity of hyperoside was mediated by catalase, which converts H_2O_2 into molecular oxygen and water (del Rio *et al*., 1992), the activity of catalase in hyperoside treated V79-4 cells were measured. Hyperoside increased catalase activity to 15.8 U/mg protein at 1 μM, 21.9 U/mg protein at 2.5 μM, and 28.5 U/mg protein at 5 μM compared to 12.4 U/mg protein in control (Fig. 3A). To confirm the activation of catalase by hyperoside in terms of protein expression, the western blot analysis was performed. As shown in Fig. 3B, in the presence of hyperoside at 5 μM, the protein expression of catalase was increased. These data suggest that hyperoside showed ROS scavenging effect and catalase activation.

A

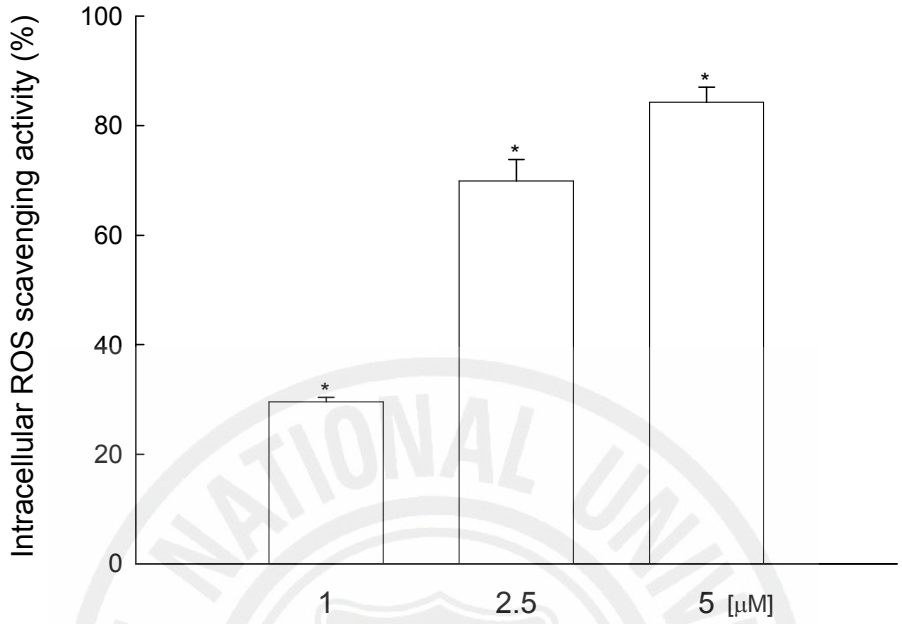

B

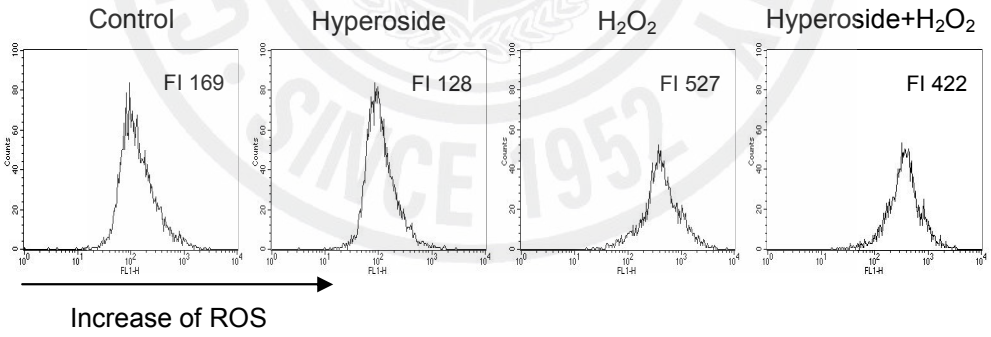

Fig. 2. Effect of hyperoside on intracellular ROS generation in H_2O_2 treated V79-4 cells.

The intracellular ROS generated was detected using spectrofluorometer (A) and using flow cytometry (B) after DCF-DA treatment. FI indicates fluorescence intensity of DCF-DA.

C

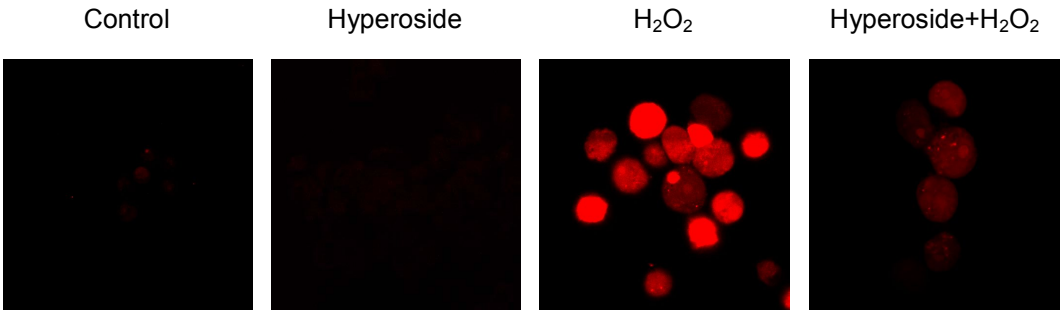

Fig. 2. continued. (C) Representative confocal images illustrate the increase in red fluorescence intensity of DCF produced by ROS in H_2O_2 treated cells as compared to control and the lowered fluorescence intensity in H_2O_2 treated cells with hyperoside (original magnification × 400). The measurements were made in triplicate and values are expressed as means ± SE.

A

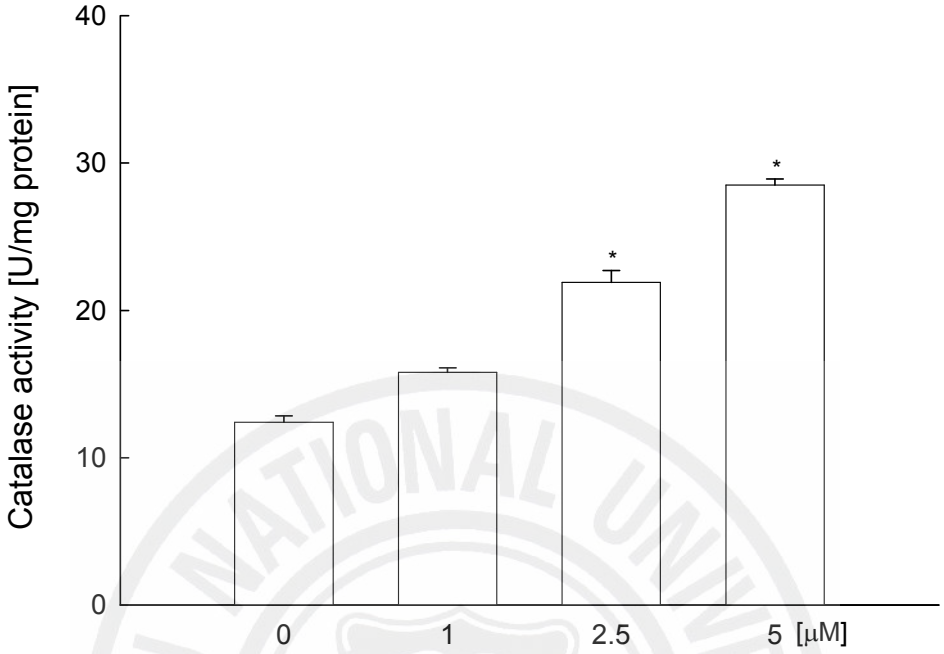

B

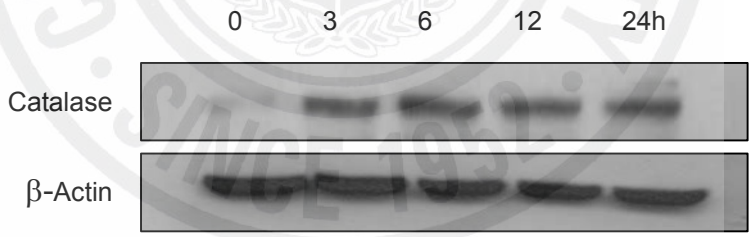

Fig. 3. Effects of hyperoside on catalase activity and its protein expression. The catalase activity (A) is expressed as average enzyme unit per mg protein ± SE. *Significantly different from control ($p<0.05$). Cell lysates were electrophoresed and the protein expression of catalase (B) was detected by a specific antibody.

2. *Effect of hyperoside on lipid peroxidation and cellular DNA damage induced by H_2O_2*

The abilities of hyperoside to inhibit membrane lipid peroxidation and cellular DNA damage in H_2O_2 treated cells were investigated. H_2O_2 induced damage to cell membrane, one of the most important lesions, responsible for the loss of cell viability. As shown in Fig. 4, V79-4 cells exposed to H_2O_2 showed an increase in the lipid peroxidation, which was monitored by the generation of TBARS. However, hyperoside prevented the H_2O_2-induced peroxidation of lipids. Damage to cellular DNA induced by H_2O_2 exposure was detected by using an alkaline comet assay, by measuring amount of 8-OHdG, and by assessing phospho histone-H2A.X expression. The exposure of cells to H_2O_2 increased the parameters of tail length and percentage of DNA in the tails of the cells. When the cells were exposed to H_2O_2, the percent of DNA in the tail increased 59%, and treatment with hyperoside resulted in a decrease to 38% as shown in Fig. 5A and B. The phosphorylation of nuclear histone H2A.X, a sensitive marker for breaks of double stranded DNA (Rogakou *et al*., 1988), increased in the H_2O_2 treated cells as shown by western blot and immuno-fluorescence results (Fig. 5C and D). However, hyperoside in H_2O_2 treated cells decreased the expression of phosphor H2A.X. 8-OHdG adduct in DNA has been used most extensively as a biomarker of oxidative stress (Tope and Panemangalore, 2007). As shown in Fig. 5E, H_2O_2 treatment increased 8-OHdG amount to 21125 pg/ml compared to 9858 pg/ml in control cells, and hyperoside treatment decreased 8-OHdG level to 12644 pg/ml, indicating a protective effect of hyperoside on H_2O_2 induced DNA damage.

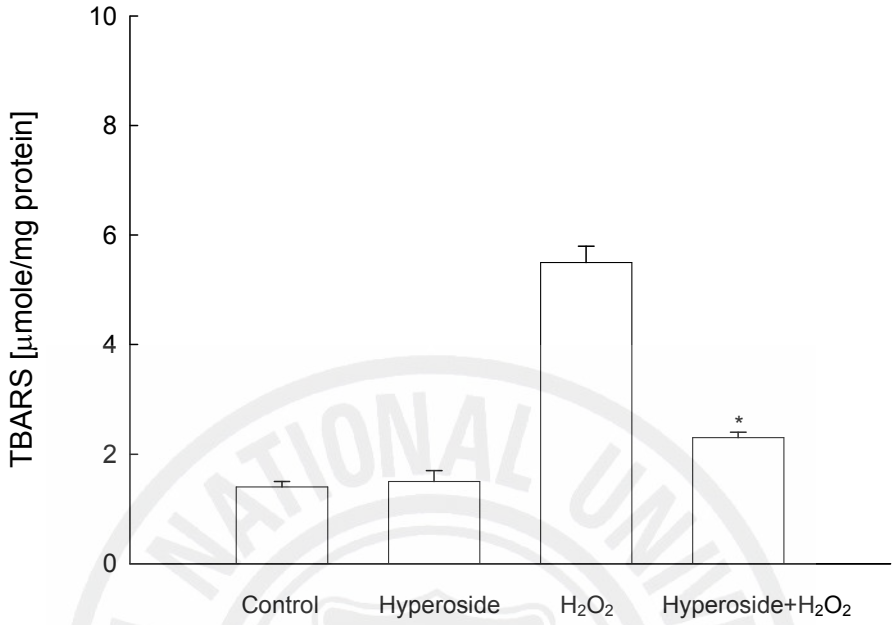

Fig. 4. Effect of hyperoside on lipid peroxidation. Lipid peroxidation was assayed by measuring the amount of TBARS formation. The measurements were made in triplicate and the values expressed as means ± SE. *Significantly different from H_2O_2 treated cells ($p<0.05$).

A

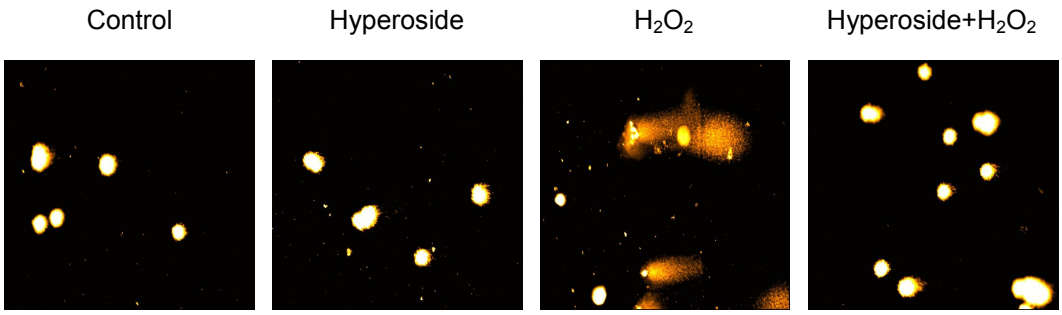

B

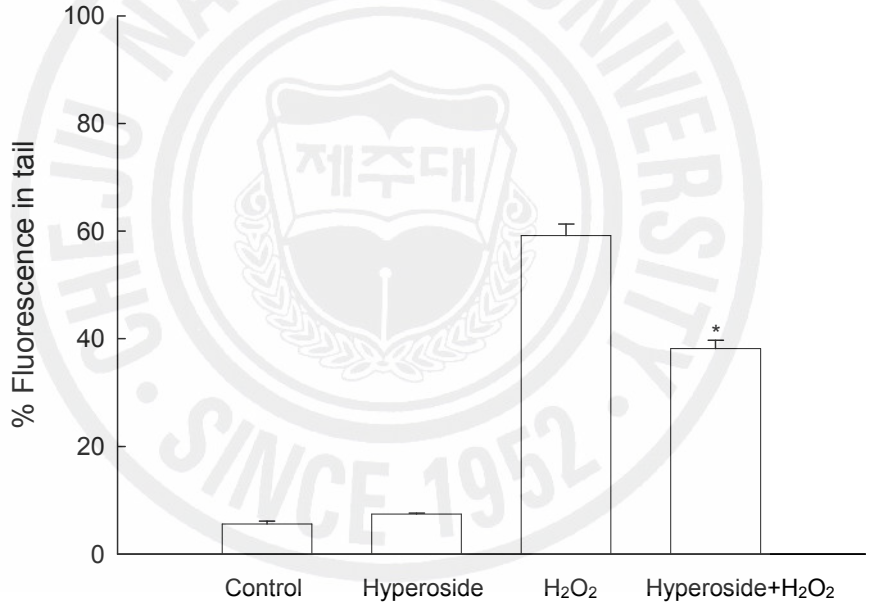

Fig. 5. Effect of hyperoside on DNA damage. (A) Representative images and (B) percentage of cellular DNA damage were detected by an alkaline comet assay. *Significantly different from H_2O_2 treated cells ($p<0.05$).

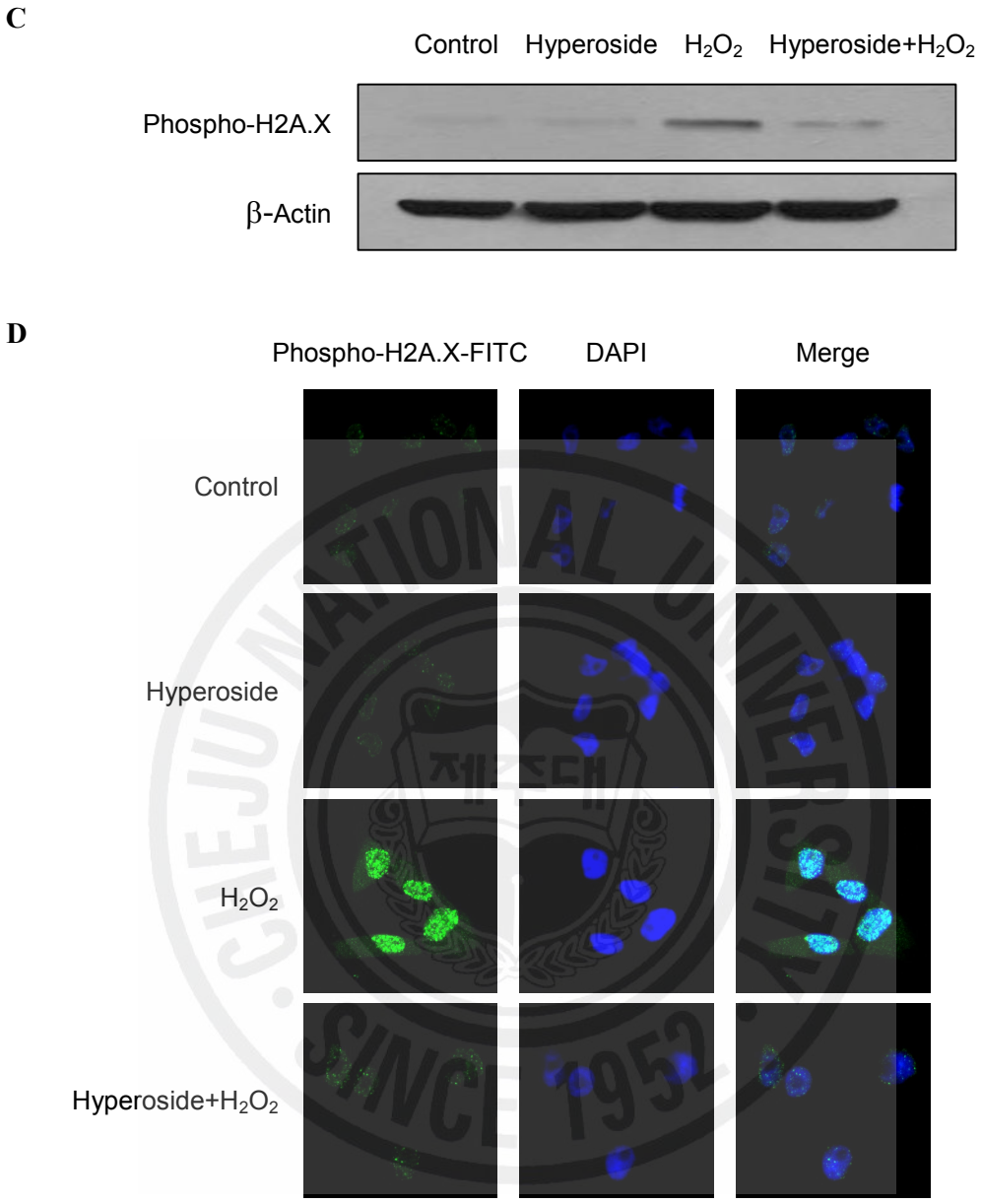

Fig. 5. continued. (C) Cell lysates were electrophoresed and phospho histone H2A.X protein was detected by specific antibody. (D) Confocal image shows that FITC-conjugated secondary antibody staining indicates the location of phospho histone H2A.X (green) by anti-phospho histone H2A.X antibody, DAPI staining indicates the location of the nucleus (blue), and the merged image indicates the location of the phospho histone H2A.X protein in nucleus.

E

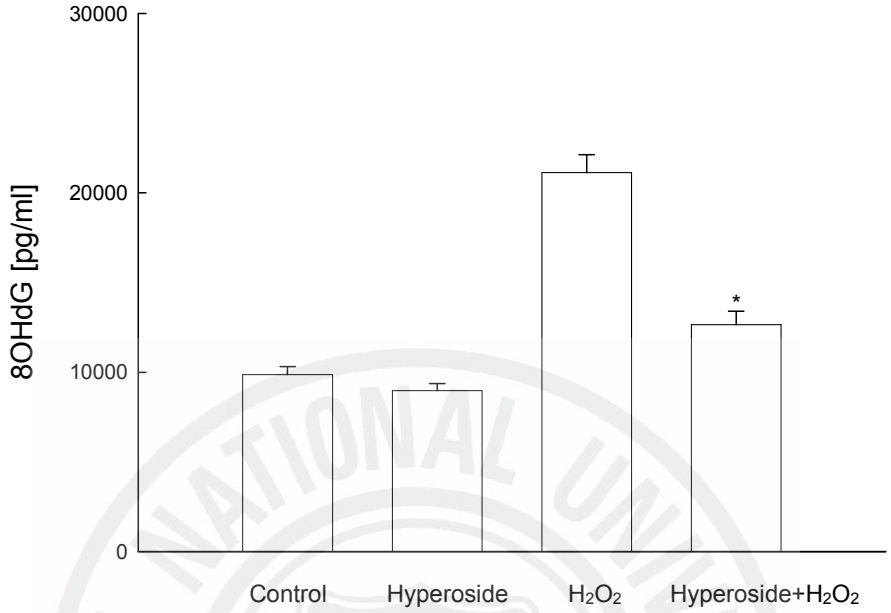

Fig. 5. continued. (E) 8-OHdG content in cellular DNA measured in ELISA kit. *Significantly different from H_2O_2 treated cells ($p<0.05$).

3. *Effect of hyperoside on apoptosis induced by H_2O_2*

The protective effect of hyperoside on cell survival in H_2O_2 treated cells was measured. Cells were treated with hyperoside at 5 μM for 1 h, prior to the addition of H_2O_2. Cell viability was determined 24 h later by the MTT assay. As shown in Fig. 6, treatment with hyperoside increased the cell survival by 56% as compared to 42% of H_2O_2 treatment. To evaluate a cytoprotective effect of hyperoside on apoptosis induced by H_2O_2, the nuclei of V79-4 cells were stained with Hoechst 33342 and assessed by microscopy. The microscopic pictures in Fig. 7A showed that the control cells had intact nuclei, while H_2O_2 treated cells showed significant nuclear fragmentation, which is characteristic of apoptosis. When the cells were treated with hyperoside for 1 h prior to H_2O_2 treatment, however, a decrease in nuclear fragmentation was observed. In addition to the morphological evaluation, the protective effect of hyperoside against apoptosis was also confirmed by apoptotic sub-G_1 DNA analysis, by ELISA based quantification of cytoplasmic histone-associated DNA fragmentation, by mitochondria membrane potential ($\Delta\psi$) analysis, and by detection of apoptosis related proteins expression. As shown in Fig. 7B, an analysis of the DNA content in the H_2O_2 treated cells revealed an increase by 65% of apoptotic sub-G_1 DNA content. Treatment with 5 μM of hyperoside decreased the apoptotic sub-G_1 DNA content to 37%. Treatment of cells with H_2O_2 increased the levels of cytoplasmic histone-associated DNA fragmentations compared to control group, however, treatment with 5 μM of hyperoside decreased the level of DNA fragmentation (Fig. 7C). H_2O_2 treatment resulted in loss of $\Delta\psi$ as observed by an increase in fluorescence (FL-1) with the dye JC-1 (Fig. 7D). Hyperoside treatment at 5 μM blocked loss of $\Delta\psi$ in response of H_2O_2 treatment. To understand the protection mechanism of hyperoside on H_2O_2 induced apoptotic process, changes in the expression of Bcl-2, an anti-apoptotic protein, and expression of Bax, a pro-apoptotic protein,

were examined. As shown in Fig. 7E, hyperoside showed the increased expression of bcl-2 and decreased expression of bax. An action of Bcl-2 during the apoptotic process is to prevent the opening of mitochondrial membrane pore and Bax is to induce the opening of membrane pore (Zamzami *et al*., 1995). It is suggest that blocked loss of $\Delta\psi$ by hyperoside treatment is resulted from up-regulation of bcl-2, and down-regulation of bax. We next examined caspase 9 activity by western blot because it is known that this enzyme is activated by mitochondrial membrane disruption (Yang *et al*., 1997). As shown in Fig. 7E, hyperoside inhibited the H_2O_2 induced activation of caspase 9 (37 kDa) and caspase 3 (17 kDa), a target of caspase 9, which is further demonstrated by the cleavage of poly ADP-ribosyl polymerase (PARP) (89 kDa). These results suggest, therefore, that hyperoside protects cell viability by inhibiting H_2O_2 induced apoptosis.

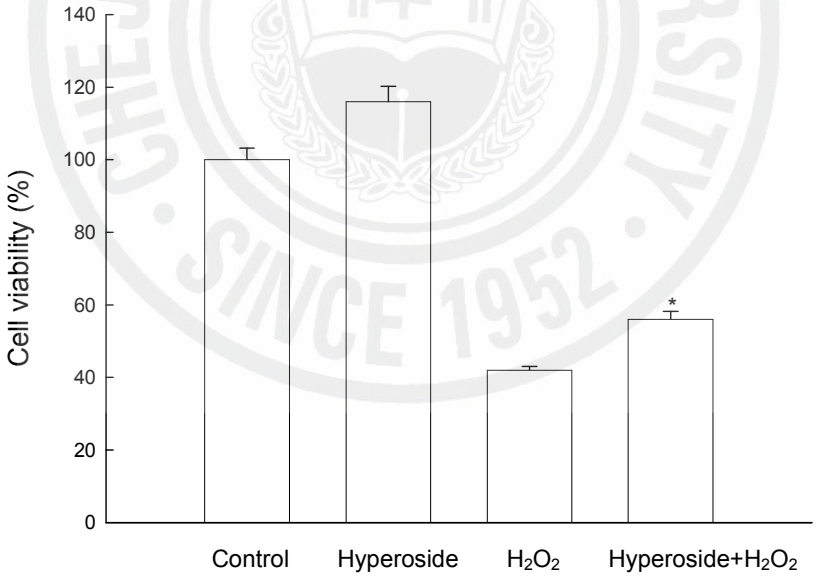

Fig. 6. Effect of hyperoside on H_2O_2 induced apoptosis. The viability of V79-4 cells on H_2O_2 treatment was determined by MTT assay. *Significantly different from H_2O_2 treated cells ($p<0.05$).

A

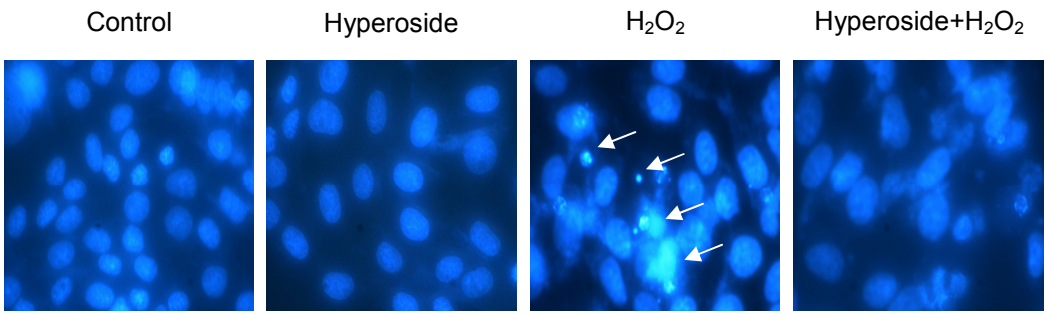

Fig. 7. Effect of hyperoside on H_2O_2 induced apoptosis. (A) Apoptotic body formation was observed under a fluorescent microscope after Hoechst 33342 staining apoptotic bodies are indicated by arrows.

B

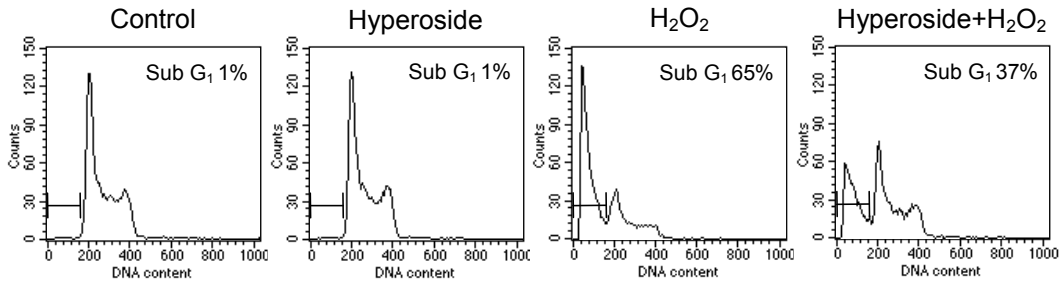

C

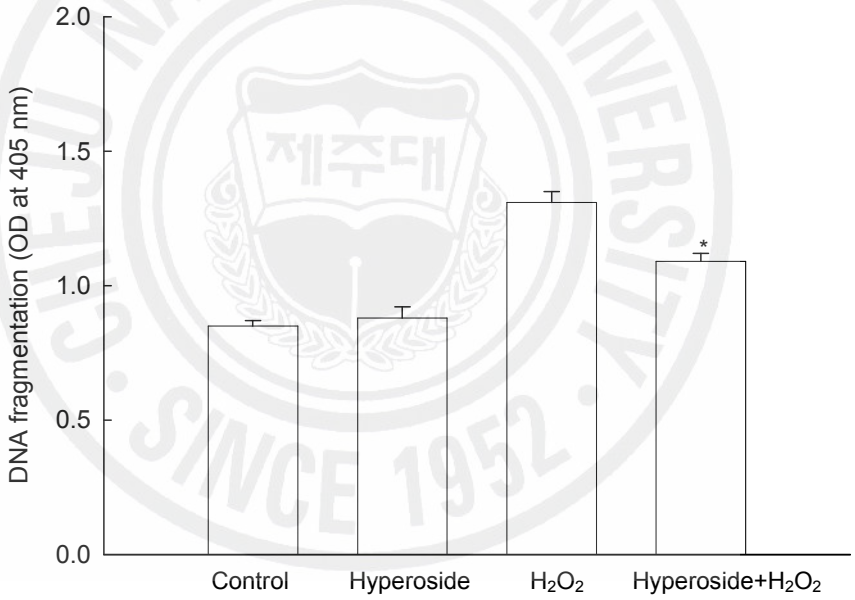

Fig. 7. continued. (B) Apoptotic sub-G_1 DNA content was detected by flow cytometry after propidium iodide staining and (C) DNA fragmentation was quantified by ELISA kit. The measurements were made in triplicate and values are expressed as means ± SE. *Significantly different from H_2O_2 treated cells ($p<0.05$).

D

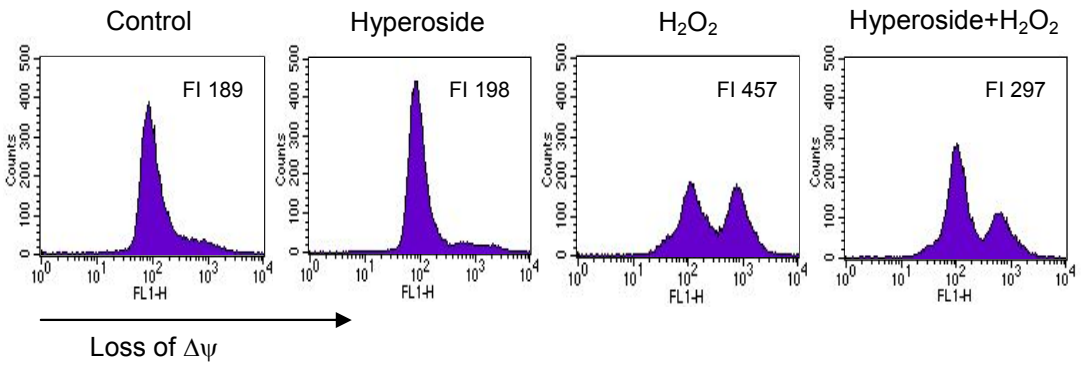

E

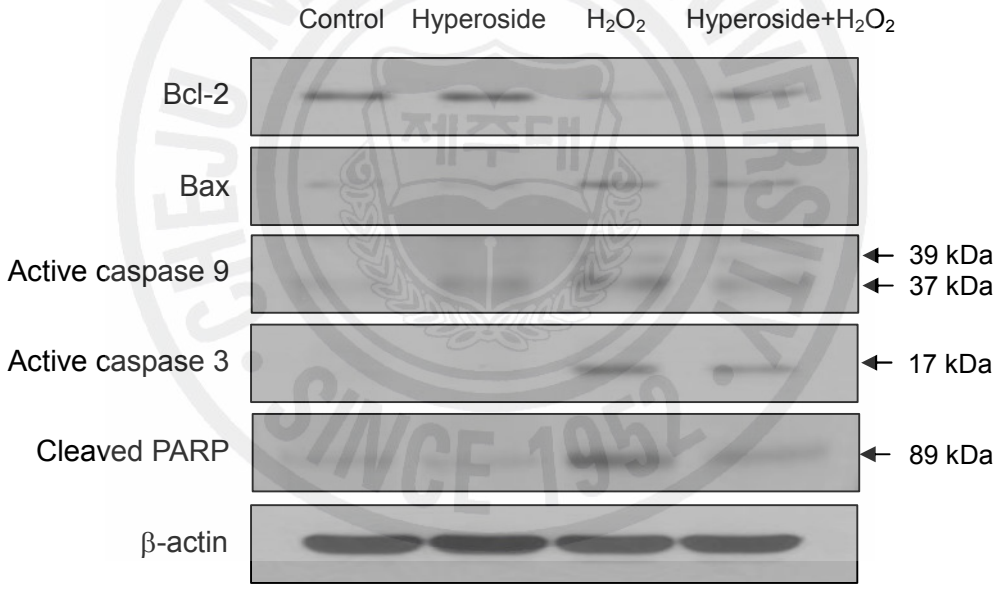

Fig. 7. continued. (D) Mitochondria membrane potential (Δψ) was analyzed by flow cytometer after staining cells with JC-1. (E) Cell lysates were electrophoresed and Bcl-2, Bax, active caspase 9, active caspase 3, and cleaved PARP proteins were detected by specific antibodies.

4. *Effects of hyperoside on H_2O_2 induced MAP kinase and AP-1 activation*

To investigate the effect of hyperoside on H_2O_2 induced MAP kinase activation, cells were pretreated with hyperoside for 3 h before the addition of H_2O_2. As shown in Fig. 8A, incubation of cells with H_2O_2 induced ERK, JNK, and p38 activation. Preincubation with hyperoside remarkably inhibited JNK activation, while the inhibition of phospho-ERK, and phospho-p38 were rather modest compared to phospho-JNK. These findings indicate that H_2O_2 induced JNK activation is most sensitive to hyperoside in V79-4 cells. AP-1 is a downstream target of the phospho-JNK pathway and activated AP-1 is involved in cell death, including apoptosis (Kitamura *et al*., 2002; Whitmarshm and Davis, 1996). We subsequently examined the effect of hyperoside on the DNA binding activity of AP-1. As shown in Fig. 8B, treatment of cells with H_2O_2 increased AP-1 DNA binding activity, and hyperoside inhibited it. The transcriptional activity of AP-1 was also assessed using a promoter construct containing the AP-1 binding DNA consensus sequences linked to a luciferase reporter gene. As illustrated in Fig. 8C, hypeorside inhibited the transcriptional activity of AP-1 induced by H_2O_2. These results suggest that hyperoside inhibits H_2O_2 induced cell death at least via suppressing JNK and AP-1 activation.

A

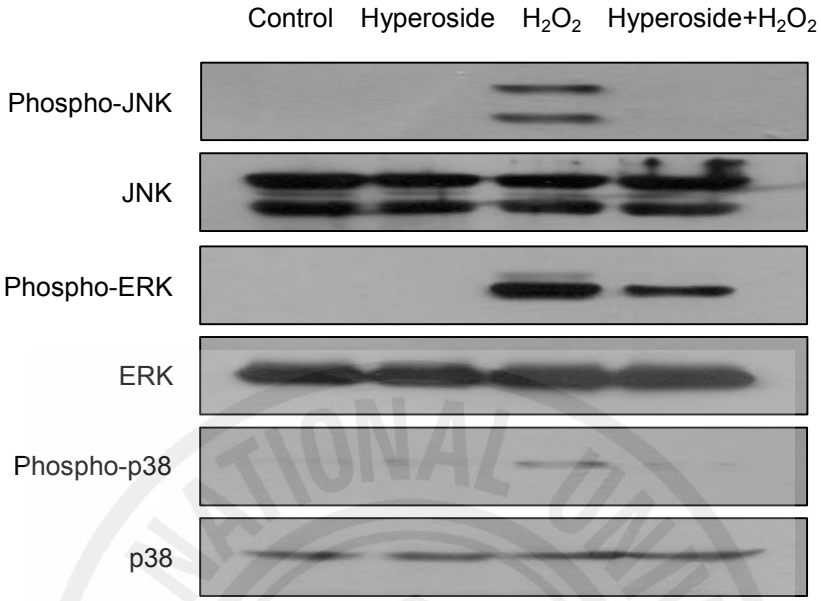

Fig. 8. Effect of hyperoside on H_2O_2 induced MAPK and AP-1 activation. (A) Cell lysates were electrophoresed and cell lysates were immunoblotted using anti-JNK, anti-phospho JNK, anti-ERK, anti-phospho ERK, anti-p38, and anti-phospho p38 antibodies.

B

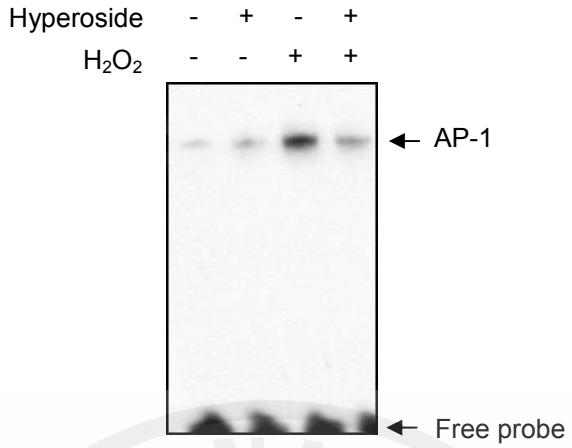

C

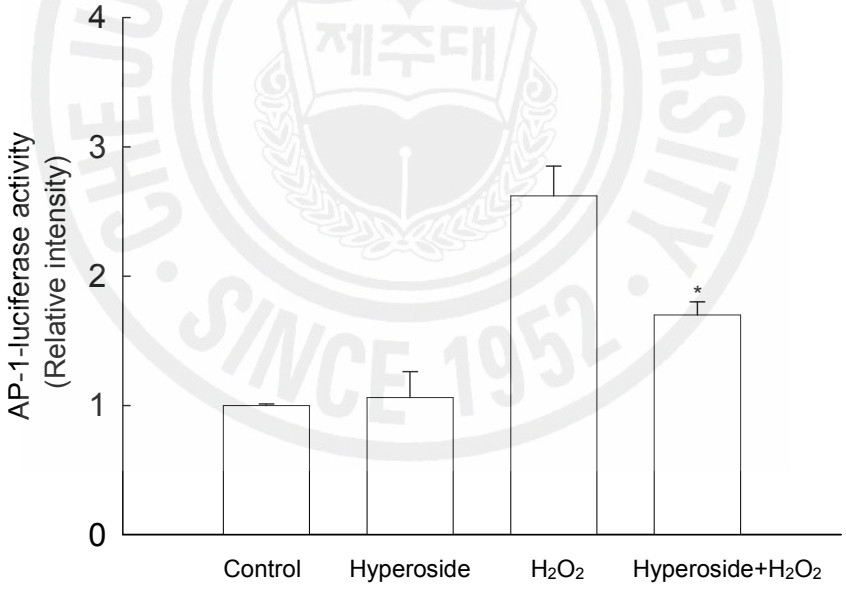

Fig. 8. continued. (B) AP-1 specific oligonucleotide-protein complexes were detected by electrophoresis mobility shift assay. (C) Transcriptional activity of AP-1 was assessed using plasmid containing the AP-1 binding site-luciferase construct.

Ⅳ. DISCUSSION

Although previous papers reported that hyperoside exhibits the antioxidant effects and cytoprotective effect against oxidative stress, there is lack of evidence supporting the inhibition of ROS formation by hyperoside and the precise mechanisms of the cytoprotective effect of hyperoside against oxidative stress (Liu *et al*., 2005). In our study, hyperoside was found to decrease the intracellular ROS and to increase catalase activity. It is reported that hyperoside permeated the cell membrane and inhibit free radical formation and the propagation of free radical reactions by chelating transition metal ions in the cells (Zou *et al*., 2004; Liu *et al*., 2005). Catalase is located at the peroxisome and converts H_2O_2 into molecular oxygen and water. Therefore, catalase plays important role in cellular protection against oxidative stress induced cell damages (Pietarinen *et al*., 1995). Our data suggests that antioxidant effects of hyperoside might be due to ROS scavenging effect and antioxidant enzyme (catalase) activation.

Hyperoside attenuated the damages of lipid membrane and DNA induced by H_2O_2, suggesting that hyperoside has cytoprotective effect. The V79-4 cells exposed to H_2O_2 exhibited the distinct features of apoptosis, such as nuclear fragmentation, sub G_1-hypodiploid cells, DNA fragmentation, disruption of mitochondrial $\Delta\psi$, activation of caspases. Cells that were pretreated with hyperoside, however, had significantly reduced percentage of apoptotic cells. These findings suggest that hyperoside inhibited H_2O_2 induced apoptosis through its ROS scavenging effect. To further analyze the molecular mechanism underlying inhibitory effect of apoptosis by hyperoside, we investigated the MAPK and AP-1 signaling pathway. Hyperoside significantly decreased the phospho form of the ERK, JNK,

and p38 kinase induced by H_2O_2 treatment. Among three types of MAPKs, the inhibition of JNK was most prominent. JNK and AP-1 activation was suggested to be critical components in the oxidative stress induced apoptosis process (Karin *et al*., 1997). Activated JNK can phosphorylate c-Jun on serine 63 and 73 (p-c-Jun), which is a component of AP-1 (Kitamura *et al*., 2002). Our EMSA data and transient transfection analysis revealed that hyperoside inhibited the AP-1 DNA binding and AP-1 mediated transcriptional activity induced by H_2O_2, suggesting that JNK and AP-1 pathway may be involved in the protective effect of hyperoside on cell apoptosis. Therefore, the cytoprotective effect of hyperoside against H_2O_2 induced apoptotic cell death appears to be mediated through inhibition of ROS generation and JNK activation.

Ⅴ. REFERENCES

Abe, J., Berk, B. C. 1998. Reactive oxygen species as mediators of signal transduction in cardiovascular disease. *Trends Cardiovasc. Med.* 8:59-64.

Carmichael, J., DeGraff, W. G., Gazdar, A. F., Minna, J. D., Mitchell, J. B. 1987. Evaluation of a tetrazolium-based semiautomated colorimetric assay: assessment of chemosensitivity testing. *Cancer Res.* 47:936-941.

Carrillo, M. C., Kanai, S., Nokubo, M., Kitani, K. 1991. (-) deprenyl induces activities of both superoxide dismutase and catalase but not of glutathione peroxidase in the striatum of young male rats. *Life Sci.* 48:517-521.

Cermak, R., Landgraf, S., Wolffram, S. 2004. Quercetin glucosides inhibit glucose uptake into brush-border-membrane vesicles of porcine jejunum. *Br. J. Nutr.* 91:849-855.

Chen, L., Li, J., Luo, C., Liu, H., Xu, W., Chen, G., Liew, O. W., Zhu, W., Puah, C. M., Shen, X., Jiang, H. 2006. Binding interaction of quercetin-3-beta-galactoside and its synthetic derivatives with SARS-CoV 3CL(pro): structure-activity relationship studies reveal salient pharmacophore features. *Bioorg. Med. Chem.* 14:8295-8306.

del Rio, L. A., Sandalio, L. M., Palma, J. M., Bueno, P., Corpas, F. J. 1992. Metabolism of oxygen radicals in peroxisomes and cellular implications. *Free Rad. Biol. Med.* 13:557-580.

Dizdaroglu, M., Jaruga, P., Birincioglu, M., Rodriguez, H. 2002. Free radical-induced damage to DNA: mechanisms and measurement. *Free Radic. Biol. Med*. 32:1102-1115.

Haddad, J. J. 2002. Science review: Redox and oxygen-sensitive transcription factors in the regulation of oxidant-mediated lung injury: role for nuclear factor-kappaB. *Crit. Care*

6:481-490.

Ishikawa, Y., Yokoo, T., Kitamura, M. 1997. c-Jun/AP-1, but not NF-kappa B, is a mediator for oxidant-initiated apoptosis in glomerular mesangial cells. *Biochem. Biophys. Res. Commun.* 240:496-501.

Jedinak, A., Maliar, T., Grancai, D., Nagy, M. 2006. Inhibition activities of natural products on serine proteases. *Phytother. Res.* 20:214-217.

Karin, M., Liu, Z., Zandi, E. 1997. AP-1 function and regulation. *Curr. Opin. Cell Biol.* 9: 240-246.

Kern, M., Tjaden, Z., Ngiewih, Y., Puppel, N., Will, F., Dietrich, H., Pahlke, G., Marko, D. 2005. Inhibitors of the epidermal growth factor receptor in apple juice extract. *Mol. Nutr. Food Res.* 49:317-328.

Kitamura, M., Ishikawa, Y., Moreno-Manzano, V., Xu, Q., Konta, T., Lucio-Cazana, J., Furusu, A., Nakayama, K. 2002. Intervention by retinoic acid in oxidative stress-induced apoptosis. *Nephrol. Dial. Transplant.* 17:84-87.

Li, S., Zhang, Z., Cain, A., Wang, B., Long, M., Taylor, J. 2005. Antifungal activity of camptothecin, trifolin, and hyperoside isolated from *Camptotheca acuminata*. *J. Agric. Food Chem.* 53: 32-37.

Liu, Z., Tao, X., Zhang, C., Lu, Y., Wei, D. 2005. Protective effects of hyperoside (quercetin-3-o-galactoside) to PC12 cells against cytotoxicity induced by hydrogen peroxide and tert-butyl hydroperoxide. *Biomed. Pharmacother*. 59:481-490.

Luo, L., Sun, Q., Mao, Y. Y., Lu, Y. H., Tan, R. X. 2004. Inhibitory effects of flavonoids from Hypericum perforatum on nitric oxide synthase. *J. Ethnopharmacol.* 93:221-225.

Madge, L. A., Li, J. H., Choi, J., Pober, J. S. 2003. Inhibition of phosphatidylinositol 3-kinase sensitizes vascular endothelial cells to cytokine-initiated cathepsin-dependent

apoptosis. *J. Biol. Chem.* 278:21295-2306.

Morris, P. E., Bernard, G. R. 1994. Significance of glutathione in lung disease and implications for therapy. *Am. J. Med. Sci.* 307:119-127.

Nguyen, C., Teo, J. L., Matsuda, A., Eguchi, M., Chi, E. Y., Henderson, W. R., Jr, Kahn, M. 2003. Chemogenomic identification of Ref-1/AP-1 as a therapeutic target for asthma. *Proc. Natl. Acad. Sci. USA*. 100:1169-1173.

Nicoletti, I., Migliorati, G., Pagliacci, M. C., Grignani, F., Riccardi, C. 1991. A rapid and simple method for measuring thymocyte apoptosis by propidium iodide staining and flow cytometry. *J. Immunol. Meth.* 139:271-279.

Ohkawa, H., Ohishi, N., Yagi, K. 1979. Assay for lipid peroxides in animal tissues by thiobarbituric acid reaction. *Anal. Biochem.* 95:351-358.

Pietarinen, P., Raivio, K., Devlin, R. B., Crapo, J. D., Chang, L. Y., Kinnula, V. L. 1995. Catalase and glutathione reductase protection of human alveolar macrophages during oxidant exposure *in vitro*. *Am. J. Respir. Cell Mol. Biol.* 13:434-441.

Prenner, L., Sieben, A., Zeller, K., Weiser, D., Haberlein, H. 2007. Reduction of High-Affinity beta(2)-Adrenergic Receptor Binding by Hyperforin and Hyperoside on Rat C6 Glioblastoma Cells Measured by Fluorescence Correlation Spectroscopy. *Biochemistry* 46:5106-5113.

Rajagopalan, R., Ranjan, S. K., Nair, C. K. 2003. Effect of vinblastine sulfate on gamma-radiation-induced DNA single-strand breaks in murine tissues. *Mutat. Res.* 536:15-25.

Rogakou, E. P., Pilch, D. R., Orr, A. H., Ivanova, V. S., Bonner, W. M. 1988. DNA double-stranded breaks induce histone H2AX phosphorylation on serine 139. *J. Biol. Chem.* 273:5858-5868.

Rosenkranz, A. R., Schmaldienst, S., Stuhlmeier, K. M., Chen, W., Knapp, W., Zlabinger, G.

J. 1992. A microplate assay for the detection of oxidative products using 2',7'-dichlorofluorescein-diacetate. *J. Immunol. Meth.* 156:39-45.

Singh, N. P. 2000. Microgels for estimation of DNA strand breaks, DNA protein cross links and apoptosis. *Mutat. Res.* 455:111-127.

Tope, A. M., Panemangalore, M. 2007. Assessment of oxidative stress due to exposure to pesticides in plasma and urine of traditional limited-resource farm workers: formation of the DNA-adduct 8-hydroxy-2-deoxy-guanosine (8-OHdG). *J. Environ. Sci. Health B* 42:151-155.

Trumbeckaite, S., Bernatoniene, J., Majiene, D., Jakstas, V., Savickas, A., Toleikis, A. 2006. The effect of flavonoids on rat heart mitochondrial function. *Biomed. Pharmacother.* 60:245-248.

Tuder, R. M., Zhen, L., Cho, C. Y. Taraseviciene-Stewart L, Kasahara Y, Salvemini D, Voelkel NF, Flores SC. 2003. Oxidative stress and apoptosis interact and cause emphysema due to vascular endothelial growth factor receptor blockade. *Am. J. Respir. Cell. Mol. Biol.* 29:88-97.

Whitmarshm A, J., Davis, R. J. 1996. Transcription factor AP-1 regulation by mitogen-activated protein kinase signal transduction pathways. *J. Mol. Med.* 74:589-607.

Wu, L. L., Yang, X. B., Huang, Z. M., Liu, H. Z., Wu, G. X. 2007. In vivo and in vitro antiviral activity of hyperoside extracted from *Abelmoschus manihot* (L) medik. *Acta. Pharmacol. Sin.* 28:404-409.

Yang, J., Liu, X., Bhalla, K., Kim, C. N., Ibrado, A. M.; Cai, J., Peng, T. I., Jones, D. P., Wang, X. 1997. Prevention of apoptosis by Bcl-2: release of cytochrome c from mitochondria blocked. *Science* 275:1129-1132.

Yang, P., He, X. Q., Peng, L., Li, A. P., Wang, X. R., Zhou, J. W., Liu, Q. Z. 2007. The role

of oxidative stress in hormesis induced by sodium arsenite in human embryo lung fibroblast (HELF) cellular proliferation model. *J. Toxicol. Environ. Health A* 70:976-983.

Yoshizumi, M., Kogame, T., Suzaki, Y., Fujita, Y., Kyaw, M.; Kirima, K., Ishizawa, K., Tsuchiya, K., Kagami, S., Tamaki, T. 2002. Ebselen attenuates oxidative stress-induced apoptosis via the inhibition of the c-Jun N-terminal kinase and activator protein-1 signalling pathway in PC12 cells. *Br. J. Pharmacol.* 136:1023-1032.

Zamzami, N., Marchetti, P., Castedo, M., Zanin, C., Vayssiere, J. L., Petit, P. X., Kroemer, G. 1995. Reduction in mitochondrial potential constitutes an early irreversible step of programmed lymphocyte death in vivo. *J. Exp. Med*. 181:1661-1672.

Zou, Y., Lu, Y., Wei, D. 2004. Antioxidant activity of a flavonoid-rich extract of Hypericum perforatum L. *in vitro*. *J. Agric. Food Chem.* 52:5032-5039.

Ⅵ. ABSTRACT IN KOREAN

이 논문은 과산화수소(H_2O_2)로 유도된 세포 사멸 및 그 메커니즘에 대한 hyperoside (quercetin-3-D-galactoside)의 세포 보호 작용을 해명하였다. Hyperoside는 세포 내 활성 산소 종 (ROS)을 소거하고 카탈라아제의 활성을 증가시킨다는 것을 발견하였다. Hyperoside는 thiobarbituric acid 반응 물질 (TBARS) 형성의 억제 작용, comet tail의 억제 작용, phospho-H2A.X 발현의 감소, 8-hydroxy-2'-deoxyguanosine (8-OHdG) 형성의 억제 작용을 나타냄으로써 지질 과산화 및 DNA 손상을 예방하였다. Hyperoside는 H_2O_2에 의하여 유도된 apoptosis의 억제 작용, 즉 apoptotic 핵 조각의 감소, sub-G1 세포 군의 감소, DNA 조각의 감소, 미토콘드리아 막 전위 ($\Delta\psi$) 손실의 억제를 통하여 중국 햄스터 폐 섬유아 (V79-4) 세포의 세포 사멸을 억제하였다. 이 보호 작용은 또 bcl-2의 up-regulation, bax의 dawn-regulation 및 caspase 9 또는 3의 비활성화 작용도 나타내었다. Hyperoside는 apoptosis와 관련되어 있는 신호 통로인 c-Jun N-terminal kinase (JNK)의 활성 및 그 하류 전사 인자, 활성 단백질-1(AP-1) 을 억제하였다. 상술한 바와 같이 이러한 연구 결과들로부터 hyperoside는 ROS의 생성 및 JNK 활성화의 억제를 통하여 H_2O_2로 유도된 V79-4 세포의 apoptosis를 억제하였음을 알 수 있었다.

Ⅶ. 감사의 글

2년 전 처음 유학 올 때는 외딴섬에 가족은커녕 친척도 친구도 아는 사람 하나 없었는데 졸업을 앞둔 지금 감사할 사람이 너무나 많아서 그 사실 조차도 감사해야 할 일인 것 같습니다.

우선 석사 과정 2년 동안, 너무나도 부족한 저를 언제나 믿어주시고 기회를 주신 현진원 교수님께 마음 깊이 감사의 말씀을 드립니다. 그리고 연구와 강의로 항상 바쁘신 가운데에도 저의 학위 논문 심사를 흔쾌히 맡아주시고 많은 조언을 해주시는 조문제 교수님과 강희경 교수님께 진심으로 감사 드립니다. 또한 언제나 상냥한 웃음으로 맞아주시고 관심과 배려를 아끼지 않는 은수용 교수님을 비롯하여 가르침을 주신 모든 교수님들께도 감사의 마음을 전하고 싶습니다.

제가 학업을 다시 시작할 수 있게 도와준 친구 미화, 한국 생활에 쉽게 적응할 수 있도록 큰 도움을 주신 안춘산 선생님께도 진심으로 감사의 마음 전하고 싶습니다.

공부, 실험, 생활 할 것 없이 항상 많은 것을 알려주고 챙겨주는 연하 선배 경아와 장예, 그 고마운 마음 이루다 말로 표현할 수 없고, 후배 동옥이와 지홍이도 같은 파트에서 배우게 된 것 만으로도 너무 고맙게 생각한다. 영미 선생님, 희경 선생님, 지은이, 진영이와는 같은 실험실에서 지내면서 많은 것을 배우고 얻었는데 신세만 지고 도움을 주지 못한 것 같아서 항상 미안한 마음이고 또 너무너무 감사합니다.

중국에서 태어나서 모국이지만 서먹한 이 땅에서 만나 동고동락 같이 하면서 지내온 연희와 금희, 지강이, 수길이, 그리고 마음을 나눌 수 있는 친구처럼 따뜻한 엘비라 선생님, 모두 진심으로 감사 드립니다. 가끔 문안을 해주는 멀리 있는 친구들... 다들 너무너무 고맙다.

마지막으로 집을 떠나 있는 저를 항상 걱정해주시고 무한한 사랑과 희생으로 보살펴 주시는 엄마, 언제나 진심어린 격려와 도움을 주는 친구 같은 남동생, 정말 너무너무 감사하고 졸업의 기쁨을 함께 나누고 싶습니다.

이 외에도 미처 언급하지 못한 고마운 분들이 너무나도 많습니다만 이름을 하나하나 되새기지 못함을 죄송하게 생각하며 모든 분들께 감사의 마음 전하고 싶습니다.